

RSC Advances



This is an *Accepted Manuscript*, which has been through the Royal Society of Chemistry peer review process and has been accepted for publication.

Accepted Manuscripts are published online shortly after acceptance, before technical editing, formatting and proof reading. Using this free service, authors can make their results available to the community, in citable form, before we publish the edited article. This *Accepted Manuscript* will be replaced by the edited, formatted and paginated article as soon as this is available.

You can find more information about *Accepted Manuscripts* in the [Information for Authors](#).

Please note that technical editing may introduce minor changes to the text and/or graphics, which may alter content. The journal's standard [Terms & Conditions](#) and the [Ethical guidelines](#) still apply. In no event shall the Royal Society of Chemistry be held responsible for any errors or omissions in this *Accepted Manuscript* or any consequences arising from the use of any information it contains.

1 **A novel sensor based on bifunctional monomers molecularly imprinted film at graphene**
2 **modified glassy carbon electrode for detecting trace of moxifloxacin**

3

4

5 Zhiming Jiang, Guangyu Li, Mingxiao Zhang*

6

7 *School of Chemistry and Chemical Engineering, Southwest University, Chong Qing 400715,*
8 *PR China*

9

10

11

12

13

14 † To whom correspondence should be addressed.

15 E-mail: pclab@swu.edu.cn

16

Abstract

A novel selective and sensitive electrochemical sensor for moxifloxacin (MFLX) detection based on bifunctional monomers molecularly imprinted polymer (MIP) membranes on a glassy carbon electrode (GCE) modified with graphene was constructed. A suspension of graphene was deposited on the GCE surface. Subsequently, a molecularly imprinted film was prepared by electropolymerization, via cyclic voltammetry of o-phenylenediamine and L-lysine as the functional monomers in the presence of MFLX as the template molecule. A control electrode (NIP) was also prepared. The electrochemical properties of the MIP and non-molecularly imprinted polymer (NIP) sensors were investigated via cyclic voltammetry (CV) and electrochemical impedance spectroscopy (EIS), in which $[\text{Fe}(\text{CN})_6]^{3-/4-}$ was used as an electrochemical active probe. The surface morphology of the imprinted film was characterized by scanning electron microscopy (SEM). The fabrication conditions that affect the performance of the imprinted sensor have been discussed. Under the optimal experimental conditions, the imprinted sensor had good linear current responses to moxifloxacin concentrations in the ranges from 1.0×10^{-9} to 1.0×10^{-8} M and 1.0×10^{-8} to 5.0×10^{-5} M, with a detection limit of 5.12×10^{-10} M ($S/N = 3$). The developed sensor was successfully applied to detect moxifloxacin in tablets and human urine samples. Moreover, the fabricated sensor possessed a good selectivity and stability, providing a promising tool for immunoassays and clinical applications.

Keywords: molecularly imprinted polymer; o-phenylenediamine; L-lysine; graphene; moxifloxacin

40 1. Introduction

41 Moxifloxacin (MFLX) is a fourth-generation fluoroquinolone antibacterial agent active
42 against a broad spectrum of Gram-positive and Gram-negative ocular pathogens, a typical
43 microorganisms and anaerobes.¹ It is mainly applied in the treatment of acute bacterial
44 sinusitis caused by sensitive microbes, acute bacterial chronic bronchitis, mild to moderate
45 community intravenous pneumonia, and skin and soft tissue infection without
46 complications.^{2,3} Moxifloxacin has been detected by various methods, such as
47 spectrophotometry,^{4,5} spectrofluorimetry,⁶ atomic absorption spectrometry,⁷ high performance
48 liquid chromatography (HPLC),⁸⁻¹¹ capillary electrophoresis (CE)¹² and electrochemical
49 methods.¹³⁻¹⁵ Electrochemical sensors, as one of the electrochemical methods, are reported as
50 ecofriendly and considered as highly sensitive, selective and convenient tool with fast
51 response and low cost as compared to the other routine analytical techniques. Various
52 electrochemical sensors have been used for the moxifloxacin determination.¹⁶⁻¹⁸ However, the
53 presence of higher concentration of some structurally related analogues such as gatifloxacin,
54 ciprofloxacin, ofloxacin and norfloxacin strongly interfere in the selective determination of
55 moxifloxacin in biological samples. Thus, the aim of this study was to prepare a sensor for the
56 selective and sensitive determination of moxifloxacin in human biological fluids.

57 As a typical approach for high affinity and specific recognition, molecularly imprinted
58 polymers (MIPs) have gained a considerable attention in the recent years and have been found
59 most promising in the field of electrochemical sensors.^{19,20} The integration of electrochemical
60 devices and MIPs, which demonstrates good sensitivity and selectivity, is an attractive
61 approach for the development of biochemical sensors.²¹⁻²³ As most MIPs commonly were
62 prepared with strategies such as bulk polymerization, precipitation polymerization and
63 sol-gels often have some limitations including slow mass transfer, incomplete template
64 removal and heterogeneous distribution of binding sites.²⁴⁻²⁶ So, the approach of
65 electropolymerization for the proper design of the MIP-modified electrode is one of the
66 efficient ways to solve these limitations by generating a rigid, uniform and compact
67 molecularly imprinted film with controlled thickness.^{27,28} For the construction of a
68 molecularly imprinted polymer (MIP)-based sensor by an electropolymerization technique,
69 the choice of functional monomer is important. The electropolymerization of
70 o-phenylenediamine (OPD) has been widely used for the preparation of molecularly
71 imprinted electrochemical sensors,^{29,30} due to its excellent biocompatibility and the feasibility
72 of immobilising different compounds. L-lysine is an essential α -amino acid with basic
73 properties. L-lysine modified electrodes have the advantages of stability and positive
74 surfaces,^{31,32} which could provide fast electron transfer. At the same time, those charged
75 molecules are more easily adsorbed on the surface of the sensor. To further increase the
76 amount of effective binding sites in the sensor, an attempt to use both of these monomers to
77 form MIP was made.

78 Although MIPs are excellent in improving selectivity, sensitivity is also a fundamentally
79 important feature of an electrochemical sensor. In some cases, MIPs resulted in a reduced
80 sensitivity. So, materials such as multi-walled carbon nanotubes (MWCNTs),^{33,34} metallic
81 nanomaterials^{35,36} and, more recently, graphene,^{37,38} have been used as a substrate layer in
82 MIPs preparation. Among these materials, graphene are considered an ideal supporting
83 material because they promote electron transfer reactions due to their significant mechanical

84 strength, high electrical conductivity, high surface area and good chemical stability.

85 Herein, for the first time, we designed a rapid, selective and sensitive sensor based on
86 MIP for the determination of moxifloxacin. The GR as a supporting material, moxifloxacin as
87 template molecule, OPD and L-lysine as the functional monomers have been used to
88 construct the MIP film on the surface of glassy carbon electrode by electropolymerization.
89 After the removal of the embedded template moxifloxacin by extraction with an 50% ethanol
90 ($V/V = 1:1$) solution, the MIP/GR/GCE sensor was finally obtained. The adsorbed
91 moxifloxacin is detected by electrochemical signal of $[\text{Fe}(\text{CN})_6]^{3-/4-}$ due to the binding of
92 moxifloxacin blocking electron transfer of $[\text{Fe}(\text{CN})_6]^{3-/4-}$ at the electrode surface. The
93 electrochemical signal intensity is related to the concentration of moxifloxacin. The whole
94 preparation procedure is shown in Scheme 1. The sensor could recognize template molecule
95 from its analogs with a good selectivity and sensitively detect moxifloxacin with a wide linear
96 range and a low detection limit. Meanwhile, the sensor was used to detect moxifloxacin in
97 real samples with satisfactory results.

98

99 2. Experimental

100 2.1. Reagents and apparatus

101 Moxifloxacin, gatifloxacin, ciprofloxacin, ofloxacin and norfloxacin were purchased
102 from Wuhan Yuancheng Gongchuang Technology Co., Ltd. (China). L-lysine was purchased
103 from Aladdin Chemical Reagent Co., Ltd. (Shanghai, China). Graphene (1.0 mg/mL) was
104 purchased from XFNANO, INC (Nanjing, China). o-phenylenediamine (OPD), potassium
105 ferricyanide, potassium ferrocyanide and ethanol were purchased from Sinopharm Chemical
106 Reagent Co. Ltd. (China). The phosphate buffer solution (PBS) was prepared by mixing stock
107 solutions of NaH_2PO_4 and Na_2HPO_4 and adjusting the pH values with either 0.10 M HCl or
108 NaOH solutions. Tablets containing moxifloxacin manufactured by Bayer Pharma AG
109 (Germany) were purchased from the local market of Chong Qing. Fresh urine samples
110 obtained from healthy person were supplied by Southwest University Hospital. All other
111 chemicals and solvents used in the experiment were of analytical grade and double distilled
112 water was used throughout the experiments.

113 Electrochemical experiments including cyclic voltammetry (CV) and differential pulse
114 voltammetry (DPV) were performed on a LK 2006AZ electrochemical workstation (Tianjin
115 Lanlike Co., Ltd., China), with a conventional three-electrode system including a
116 MIP/GR/GCE as working electrode, a Pt wire counter electrode and a saturated calomel
117 electrode (SCE) reference electrode. All potential values given below were referred to the
118 SCE. The scanning electron micrograph (SEM) measurement was carried out on scanning
119 electron microscope (JSM-6510, Japan). Electrochemical impedance spectroscopy (EIS) was
120 performed on a CHI 660D electrochemical workstation (Chenhua Corp. Shanghai, China). A
121 digital pH/mV/Ionmeter (CyberScan model 2500, USA) was used for the preparation of the
122 buffer solution.

123 2.2. Preparation of the graphene-modified electrode

124 The bare GCE (3 mm in diameter) was polished with $0.05 \mu\text{m}$ Al_2O_3 slurry before it was
125 used, and rinsed ultrasonically with 1:1 HNO_3 , ethanol and ultrapure water respectively until
126 a mirror-like surface was obtained. The electrode was then washed with ultrapure water and
127 allowed to dry at room temperature before use. Two microliters of the graphene suspension

128 (1.0 mg/mL) was dropped onto the surface of the GCE and dried in the vacuum oven at 60 °C
129 for 1 h.

130 2.3. Construction of the MIP/GR/GCE, MIP/GCE and NIP/GR/GCE

131 The GR/GCE was immersed in 10.0 mL phosphate buffer solution (pH = 5.7) containing
132 1.0 mM OPD and 1.0 mM L-lysine as the functional monomers, and 0.10 mM of template
133 moxifloxacin and was electrochemically polymerized via cyclic voltammetry (CV) in the
134 potential range of -0.2 to 0.8 V at a scan rate of 50 mV/s for 20 cycles. After the
135 electropolymerization, the polymers modified electrode was incubated into an 50% ethanol
136 (V/V = 1:1) solution for 3 min to extract the template moxifloxacin to obtain the
137 MIP/GR/GCE. The procedure for the preparation of the MIP/GR/GCE is depicted in Scheme
138 1. As a control, none-imprinted polymer sensor (NIP/GR/GCE) and MIP/GCE were prepared
139 by the same procedure but without the addition of moxifloxacin and GR, respectively.

140 2.4. Electrochemical characterization and measurements

141 Different modified electrodes were characterized by EIS in a solution of 5.0 mM
142 $K_3[Fe(CN)_6]/K_4[Fe(CN)_6]$ (1:1) containing 0.10 M KCl using an alternating current voltage of
143 10 mV and recorded at a bias potential of 200 mV within a frequency range of 10^{-1} to 10^5 Hz.

144 $[Fe(CN)_6]^{3-}/[Fe(CN)_6]^{4-}$ was also chosen as an electrochemical active probe to study the
145 performance of the prepared sensor due to the poor electroactivity of moxifloxacin. Imprinted
146 cavities formed in the MIP/GR could provide pathway for the diffusion of probe into and out
147 of the MIP matrix, which then is oxidized or reduced at the electrode and produce an
148 electrochemical signal. The MIP/GR/GCE was immersed into moxifloxacin solution with
149 different concentrations, and incubated for 10 min to ensure moxifloxacin molecule rebound
150 by MIP/GR/GCE. Then, CV and DPV methods were conducted for electrochemical
151 determination of moxifloxacin in 2.0 mM $[Fe(CN)_6]^{3-/4-}$ containing 0.10 M KCl (pH = 7.0).
152 CV was performed over a potential range from -0.2 to 0.6 V with a scan rate of 100 mV/s.
153 DPV measurement was carried out between -0.2 and 0.6 V, pulse width 50 ms, and an
154 amplitude of 50 mV. All the electrochemical experiments were conducted at room
155 temperature (RT, 25 ± 1 °C).

156 2.5. Preparation and determination of real samples

157 A proposed sensor for evaluating the accuracy of the content of moxifloxacin in
158 commercial tablets (400 mg of moxifloxacin in each tablet, from Bayer Pharma AG) was
159 determined using the DPV method. Ten tablets of moxifloxacin drug were accurately weighed
160 in order to find the average weight of each tablet. Then, the tablets were powdered in a mortar
161 and carefully mixed. A quantity equivalent to one tablet was weighed, dissolved into double
162 distilled water and transferred to a 100 mL volumetric flask, and diluted to the mark with
163 double distilled water. The resulting solution was centrifuged at 5000 rpm; then, the
164 supernatant was collected and diluted to 100 mL and used as a stock solution of the sample.

165 Urine samples were collected in sterile bottles. The samples were spiked with known
166 concentration of moxifloxacin, centrifuged (3000 rpm, 10 min) to removal of proteins and
167 diluted to 50% with 0.10 M phosphate buffer solution (pH = 7.0). The samples were then
168 analysed without further treatment, using the conditions described in Section 2.4.

169

170 3. Results and discussion

171 3.1. Characterization of the different modified electrodes

172 SEM was performed to obtain an insight into the surface morphology of the different
173 modified electrodes, as shown in Fig. 1. Fig. 1A–C shows the SEM of GR/GCE,
174 MIP/GR/GCE, and NIP/GR/GCE, respectively. Fig. 1A can be realized from the images that
175 GR has large surface area which makes it easy for the electron transfer. It can be found rough
176 and multihole structure in Fig. 1B, which provided a large recognition sites in removing the
177 MIP/GR/GCE. However, there are no imprinted cavities in removing the NIP/GR/GCE.

178 The extraction of moxifloxacin from the MIP layer on the surface of electrode has
179 resulted in the formation of imprinted cavities in the MIP/GR/GCE. The formed imprinted
180 cavities could act as channels and allow access for the diffusion of $[\text{Fe}(\text{CN})_6]^{3-/4-}$ into and out
181 of the polymeric network, which could be oxidized or reduced at the electrode and produce an
182 electrochemical signal. As an effective method for probing the features of a surface modified
183 electrode, electrochemical impedance spectroscopy (EIS) was employed to characterize the
184 stepwise construction process of the sensor. Fig. 2A shows the EIS curves of different
185 electrodes. Bare GCE (a) shows a very low charge transfer resistance. With the modification
186 of the MIP before elution (b), the resistance to charge transfer (R_{ct}) is large because the film
187 modified on the electrode is nonconductive. When the template moxifloxacin was removed
188 out of the imprinted film (c), the R_{ct} reduced significantly, which suggested that the removal
189 of moxifloxacin from the MIP film decrease the electron transfer resistance. This
190 phenomenon could be attributed to the formation of imprinted cavities after the removal of
191 template moxifloxacin, leaving channels for the penetration of $[\text{Fe}(\text{CN})_6]^{3-/4-}$ through the MIP
192 film to reach GCE for the further oxidation. The R_{ct} of MIP/GR/GCE after elution (d) is less
193 than that of MIP/GCE after elution (c), which verifies that the graphene facilitates electron
194 transfer. Compared with MIP/GR/GCE after elution (d), the NIP/GR/GCE after elution (e)
195 shows larger diameter semicircle which relates to the presence of template moxifloxacin.

196 The current change of $[\text{Fe}(\text{CN})_6]^{3-/4-}$ on the different electrodes recorded by CV method
197 confirmed the same result. As shown in Fig. 2B, the MIP/GCE (b) before elution hardly has
198 current response. After removal of the template, the current response of MIP/GCE (c)
199 increases, which suggests that the cavities are formed in the MIP membranes. The current
200 response of the CV of the $[\text{Fe}(\text{CN})_6]^{3-/4-}$ at the MIP/GR/GCE (d) is larger than that of
201 MIP/GCE (c) after the addition of graphene. Graphene shows high conductivity which allows
202 $[\text{Fe}(\text{CN})_6]^{3-/4-}$ to reach the electrode surface easily. Compared with the MIP/GR/GCE (d), the
203 NIP/GR/GCE (e) without the template has very small current response. The results might be
204 attributed to the NIP membranes that block the electron transfer.

205 3.2. Choice of electropolymerized monomer for MIP/GR/GCE

206 In order to choose an efficient monomer, OPD, L-lysine, and OPD–lysine were
207 employed as different monomer to prepare three sensors and the specific rebinding properties
208 were investigated. From Fig. S2, sensor prepared using OPD or L-lysine as monomer showed
209 the specific adsorption since the current of $[\text{Fe}(\text{CN})_6]^{3-/4-}$ on NIP/GR/GCE was really low,
210 implying that the OPD or L-lysine could be applied individually in the MIP preparation for
211 determination of moxifloxacin. The sensor prepared using OPD and L-lysine as monomer
212 showed the highest current of $[\text{Fe}(\text{CN})_6]^{3-/4-}$ compared with other sensors, which could be
213 explained that the synergistic effects of OPD and L-lysine in MIP film could rebind lots of
214 moxifloxacin molecules. The imprinted factors (IF, $\text{IF} = \Delta I_{\text{MIPs}}/\Delta I_{\text{NIPs}}$) have been calculated
215 and compared on the three kinds of sensors, which were 2.6, 5.5, and 10.2, corresponding to

216 the sensors prepared using L-lysine, OPD, and OPD-lysine as monomer, respectively. These
217 results fully illustrated the advantage of OPD-lysine as a polymerized monomer.

218 3.3. Optimization of conditions for MIP/GR/GCE preparation

219 3.3.1 Effect of the volume of graphene suspension

220 The effect of volume of graphene suspension on the peak current in the MIP/GR/GCE
221 was initially studied. As shown in Fig. S3(A), the $[\text{Fe}(\text{CN})_6]^{3-/4-}$ current responses increased
222 from 0 to 2.0 μL and then decreased sharply with further increase of the graphene volume. A
223 large volume of graphene on the GCE can increase the sensor response. However, an increase
224 of the graphene volume to above the threshold value leads to a decrease, probably because of
225 the thick graphene membrane which decreases the electrode surface conductivity.

226 3.3.2 Effect of function monomer to template ratio

227 The monomer concentration in the electropolymerization process could affect not only
228 the thickness of the polymer matrix but also the amount of imprinted molecule, which in turn
229 influences the electrochemical behavior of the sensor. To investigate the effect of monomer
230 concentration on the MIP/GR/GCE, the electrodes were electropolymerized in different
231 monomer concentrations in the range of 0.80–2.0 mM with a constant moxifloxacin
232 concentration of 0.10 mM. As shown in Fig. S3(B), the highest peak current of $[\text{Fe}(\text{CN})_6]^{3-/4-}$
233 on the MIP/GR/GCE was observed when the concentration of monomer was at 1.0 mM. A
234 lower peak current was found when monomer concentration was lower than 1.0 mM, which
235 may be due to the less capture of moxifloxacin during electropolymerization. Additionally, a
236 considerable decrease in the current response on MIP/GR/GCE was observed when the
237 concentration of monomer was above 1.0 mM because the electropolymerized film was too
238 compact to form imprinted caves after elution. Thus, the optimum concentration of monomer
239 for preparing MIP/GR/GCE was 1.0 mM.

240 3.3.3 Scan cycles and scan rate of electropolymerization

241 Scan cycles and scan rate of electropolymerization are both important factors for the
242 fabrication of MIP/GR/GCE, which would influence the thickness and compactness of the
243 imprinted polymers, respectively. To investigate the effect of scan cycles on the polymer
244 thickness, 5–30 scan cycles were carried out. From the results of Fig. S3(C), higher cycles
245 lead to thicker films with less accessible imprinted sites. The optimum polymerization cycles
246 was selected as 20 according to the peak current of $[\text{Fe}(\text{CN})_6]^{3-/4-}$. Fig. S3(D) showed the
247 influence of scan rate on electropolymerization. On the one hand, at a slower scan rate the
248 imprinted polymer formed a tight polymer that decreased the accessibility of removing
249 template moxifloxacin to form imprinted sites. On the other hand, a loose and rough film with
250 a low recognition capacity was formed at a faster scan rate. Thus, the optimum scan rate of
251 electropolymerization was set to be 50 mV/s.

252 3.3.4 Template removal treatment

253 To remove the template molecules completely is a very important step in the preparation
254 of molecularly imprinted electrochemical sensors. An 50% ethanol ($V/V = 1:1$) solution was
255 used to elute the template molecules. $[\text{Fe}(\text{CN})_6]^{3-/4-}$ was used as a probe molecule and
256 scanned the differential pulses corresponding to different elution times. Fig. S3(E) is the
257 elution curve of the MIP/GR/GCE. As shown in Fig. S3(E), as the elution time increased, the
258 current gradually increased until it approached a stable value after more than 3 min of the
259 elution time. It indicated that the template molecules were removed completely from the MIP.

260 So we choose an 50% ethanol ($V/V = 1:1$) solution and 3 min as the best solvent and time for
261 template removal. Fig. S3(F) is the elution curve of the MIP/GCE. Compared with the
262 MIP/GCE, the current response of MIP/GR/GCE after elution is larger. The results further
263 indicated that graphene could improve the conductivity of molecularly imprinted polymers.

264 3.4. Optimization of determination conditions

265 3.4.1 The pH effect of rebinding solution for MIP/GR/GCE

266 The pH effect of rebinding solution was investigated by DPV method at constant
267 concentration of moxifloxacin (1.0×10^{-8} M) in PBS with the pH value ranging from 5.7 to 7.4.
268 As shown in Fig. S4(A), the response current increased from pH 5.7 to 6.5 and decreased
269 above pH 6.5. The highest current changes (ΔI) of $[\text{Fe}(\text{CN})_6]^{3-/4-}$ was observed when the pH
270 value of rebinding solution was adjusted to 6.5. Thus, we chose the pH value as 6.5.

271 3.4.2 The effect of incubation time

272 The incubation time is important for the sensitivity of the sensor. After removal of
273 template molecule, the MIP/GR/GCE was incubated in 4.0×10^{-9} M moxifloxacin solution at
274 different times. The test results are shown in Fig. S4(B). The peak current decreased sharply
275 with the incubation time from 0 to 15 min, which indicates the rapid and effective recognition
276 ability of the MIP film for the target molecule. When the incubation time reached 10 min, the
277 oxidation peak current levelled off gradually. So 10 min was chosen as the incubation time in
278 this experiment.

279 3.5. Electrochemical behavior of the electrochemical active probe

280 The electrochemical mechanism can usually be obtained from the relationship between
281 the peak current and the scan rate. The CV curves of the imprinted sensors in the
282 $[\text{Fe}(\text{CN})_6]^{3-/4-}$ solution at different scan rates were investigated in the range of 10–100 mV/s.
283 As seen in Fig. S5, the peak currents of the CV in the imprinted sensor increased with the
284 increment of the scan rate. The anodic (I_{pa}) and cathodic (I_{pc}) peak currents were nearly
285 independent of the scan rate and can be expressed as: I_{pa} (μA) = $8.51 + 5.17v^{1/2}$ ($R^2 = 0.998$)
286 and I_{pc} (μA) = $-9.40 - 4.03v^{1/2}$ ($R^2 = 0.998$) (where v is the scan rate with units mV/s),
287 suggesting typical surface controlled electrochemical behavior.

288 3.6. Calibration curve

289 Under the optimum conditions, the detection of various concentrations of moxifloxacin
290 was investigated with DPV using the MIP/GR/GCE sensor. As shown in Fig. 3, the peak
291 current decreased as the moxifloxacin concentration increased, and the reduction in ΔI for
292 $[\text{Fe}(\text{CN})_6]^{3-/4-}$ was proportional to the moxifloxacin concentrations for the ranges
293 1.0×10^{-9} – 1.0×10^{-8} M and 1.0×10^{-8} – 5.0×10^{-5} M, respectively. The linear regression equations
294 are: ΔI (μA) = $11.3 \log C_{\text{MFLX}} (\text{M}) + 106.3$ ($R^2 = 0.998$) and ΔI (μA) = $1.59 \log C_{\text{MFLX}} (\text{M}) +$
295 28.81 ($R^2 = 0.997$). The imprinted sensor had a detection limit ($S/N = 3$) of 5.12×10^{-10} M for
296 moxifloxacin. Table S1 shows the comparison of the performance of this sensor with other
297 sensors for moxifloxacin detection. The results indicated that the prepared MIP/GR/GCE
298 possessed an excellent sensitivity and a high selectivity for moxifloxacin determination.

299 3.7. Repeatability and stability

300 To evaluate the reproducibility of the MIP/GR/GCE sensor, the net response of the
301 sensor before and after incubation in 1.0×10^{-8} M moxifloxacin solution was measured with
302 five replicates. The relative standard deviation (RSD) was 1.2% for the five successive assays.
303 On the other hand, five sensors were prepared and tested under the same conditions, and the

304 RSD of five tests was 3.3%. Furthermore, the storage stability of the sensor was investigated.
305 The results showed that the sensor lost only 6.0% of its initial response after it was stored in
306 refrigerator for 25 days. Therefore, the MIP/GR/GCE sensor has good reproducibility and
307 stability.

308 3.8. Selectivity

309 The selectivity of sensor towards moxifloxacin (MFLX) was evaluated by DPV using
310 compounds with structures similar to moxifloxacin such as gatifloxacin (GFLX),
311 ciprofloxacin (CPLX), ofloxacin (OFLX) and norfloxacin (NFLX). As shown in Fig. S1, the
312 current variation (ΔI) ($\Delta I = I_0 - I_c$, where I_0 is the original current and I_c denotes the current
313 response of MIP/GR/GCE incubated in a solution of concentration) of MIP/GR/GCE was
314 higher than that at NIP/GR/GCE. The current response of the sensor to different analytes was
315 measured at a concentration of 4.0×10^{-9} M. It is found that the sensor had stronger response
316 towards moxifloxacin template than those structurally related analogues, suggesting that the
317 sensor had special recognition and selectivity to moxifloxacin due to the imprinted effect. The
318 imprinting and selecting factors are defined as

319

$$320 \alpha = (\Delta I/I_0)_{\text{MIP}}/(\Delta I/I_0)_{\text{NIP}} \quad (1)$$

321

$$322 \beta = \alpha_{\text{MFLX}}/\alpha_{\text{analog}} \quad (2)$$

323

324 where the α value of the sensor to template molecule is much higher than that to the other
325 substances. The calculated results are given in Table S2, which suggest that the size and the
326 conformation of cavities match with moxifloxacin in the MIP network.

327 3.9. Applications

328 The sensor was evaluated by carrying out the determination of moxifloxacin in the real
329 samples solution obtained from tablets and human urine samples using the standard addition
330 method under optimized conditions. The moxifloxacin content of real samples was
331 determined using the MIP/GR/GCE, and the results were shown in Table 1. The recoveries of
332 96–103% and the relative standard deviation less than 2.0% for the proposed sensor in real
333 sample analysis indicate the acceptable precision for the voltammetric determination of
334 moxifloxacin using the MIP sensor. Therefore, the MIP/GR/GCE is successfully applied to
335 the monitoring of moxifloxacin in biological and pharmaceutical samples.

336

337 4. Conclusions

338 In this study, we have developed a new electrochemical sensor for moxifloxacin
339 determination using a novel graphene-molecular imprinted polymers composite as recognition
340 element. There are several advantages of the developed MIP/GR/GCE sensor. First,
341 preparation of MIP/GR/GCE sensor simply involved electrochemical polymerization of
342 o-phenylenediamine and L-lysine, in the presence of moxifloxacin on the surface of GR/GCE,
343 which was really convenient and inexpensive. Second, the resultant MIP/GR/GCE sensor can
344 selectively recognize the template moxifloxacin and revealed a remarkably wide linear range
345 with a low detection of limit down to 5.12×10^{-10} M. Third, short response periods,
346 satisfactory reproducibility and stability were also demonstrated. Moreover, MIP/GR/GCE
347 sensor has been successfully used to determine moxifloxacin in real samples with satisfactory

348 results.

349

350 **Appendix A. Supporting information**

351 Supplementary data associated with this article can be found in the supporting information.

352

353 **References**

- 354 1 A. P. de Miranda, C. B. Silva, L. M. J. Mimica, B. K. Moscovici, G. R. Malavazzi and R. Y.
355 Hida, *J. Cataract Refr. Surg.*, 2015, **41**, 135–139.
- 356 2 W. Khan, K. L. Sullivan, J. W. McCann, C. F. Gonsalves, T. Sato and D. J. Eschelmann, *Am.*
357 *J. Roentgenol.*, 2011, **197**, 343–345.
- 358 3 I. C. Gyssens, M. Dryden, P. Kujath, D. Nathwani, N. Schaper and B. Hampel, *J.*
359 *Antimicrob. Chemother.*, 2011, **66**, 2632–2642.
- 360 4 S. K. Motwani, S. Chopra, F. J. Ahmad and R. K. Khar, *Spectrochim. Acta A*, 2007, **68**,
361 250–256.
- 362 5 A. A. Elbashir, S. A. Ebraheem, A. H. Elwagee and H. Y. Aboul-Enein, *Acta Chim. Slov.*,
363 2013, **60**, 159–165.
- 364 6 M. Kamruzzaman, A. M. Alam, S. H. Lee, D. Ragupathy, Y. H. Kim, S. R. Park and S. H.
365 Kim, *Spectrochim. Acta A*, 2012, **86**, 375–380.
- 366 7 S. M. Al-Ghannam, *Spectrochim. Acta A*, 2008, **69**, 1188–1194.
- 367 8 Y. H. Xu, D. Li, X. Y. Liu, Y. Z. Li and J. Lu, *J. Chromatogr. B*, 2010, **878**, 3437–3441.
- 368 9 A. K. Kumar, V. Sudha, R. Srinivasan and G. Ramachandran, *J. Chromatogr. B*, 2011, **879**,
369 3663–3670.
- 370 10 B. Raju, M. Ramesh, R. M. Borkar, R. Padiya, S. K. Banerjee and R. Srinivas, *Biomed.*
371 *Chromatogr.*, 2012, **26**, 1341–1347.
- 372 11 A. D. Pranger, J. W. Alffenaar, A. M. Wessels, B. Greijdanus and D. R. Uges, *J. Anal.*
373 *Toxicol.*, 2010, **34**, 135–141.
- 374 12 L. A. Cruz and R. Hall, *J. Pharm. Biomed. Anal.*, 2005, **38**, 8–13.
- 375 13 A. E. Radi, T. Wahdan, Z. Anwar and H. Mostafa, *Drug Test Anal.*, 2010, **2**, 397–400.
- 376 14 A. G. T. Magno, M. S. Glaucia and S. F. Valdir, *Microchem. J.*, 2005, **81**, 209–216.
- 377 15 N. Erk, *Anal. Bioanal. Chem.*, 2004, **378**, 1351–1356.
- 378 16 Q. Zhou, N. Long, L. Liu, H. Zhai and M. Zhu, *Int. J. Electrochem. Sci.*, 2015, **10**,
379 5069–5076.
- 380 17 M. M. Hefnawy, A. M. Homoda, M. A. Abounassif, A. M. Alanazi, A. Al-Majed and G. A.
381 Mostafa, *Chem. Cent. J.*, 2014, **8**, 59–66.
- 382 18 A. Radi, T. Wahdan, Z. Anwar and H. Mostafa, *Electroanal.*, 2010, **22**, 2665–2671.
- 383 19 K. Haupt and K. Mosbach, *Chem. Rev.*, 2000, **100**, 2495–2504.
- 384 20 L. Ye and K. Mosbach, *Chem. Mater.*, 2008, **20**, 859–868.
- 385 21 Z. Wang, F. Li, J. Xia, L. Xia, F. Zhang, S. Bi, G. Shi, Y. Xia, J. Liu, Y. Li and L. Xia,
386 *Biosens. Bioelectron.*, 2014, **61**, 391–396.
- 387 22 Q. Tang, X. Shi, X. Hou, J. Zhou and Z. Xu, *Analyst*, 2014, **139**, 6406–6413.
- 388 23 J. Ji, Z. Zhou, X. Zhao, J. Sun and X. Sun, *Biosens. Bioelectron.*, 2015, **66**, 590–595.
- 389 24 N. Sallacan, M. Zayats, T. Bourenko, A. B. Kharitonov and I. Willner, *Anal. Chem.*, 2002,
390 **74**, 702–712.
- 391 25 F. L. Dickert, M. Tortschanoff, W. E. Bulst and G. Fischerauer, *Anal. Chem.*, 1999, **71**,

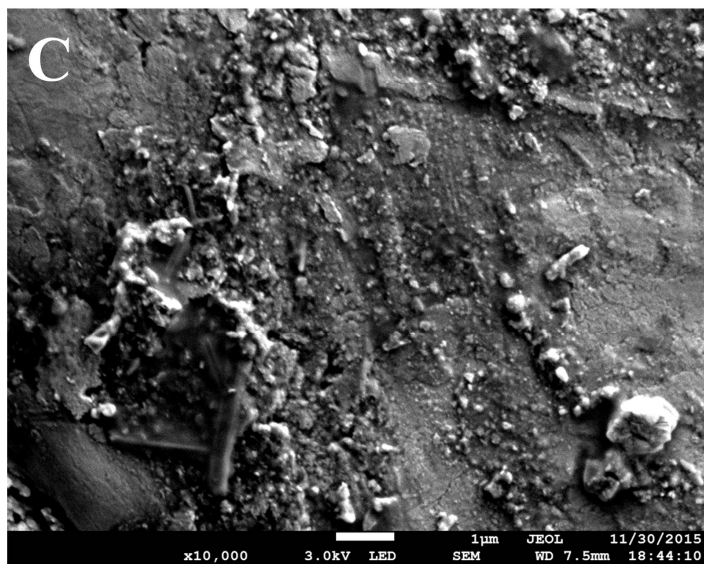
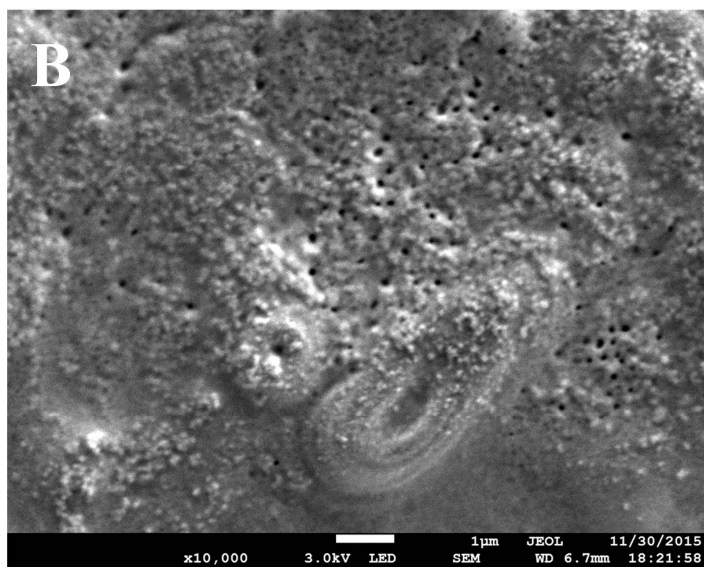
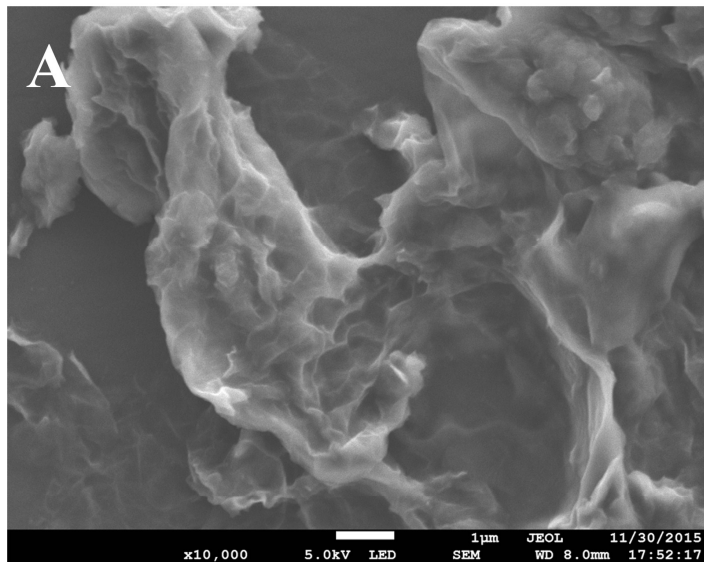
- 392 4559–4563.
- 393 26 S. C. Zimmerman, M. S. Wendland, N. A. Rakow, I. Zharov and K. S. Suslick, *Nature*,
394 2002, **418**, 399–403.
- 395 27 W. Lian, S. Liu, J. Yu, X. Xing, J. Li, M. Cui and J. Huang, *Biosens. Bioelectron.*, 2012, **38**,
396 163–169.
- 397 28 Y. T. Liu, J. Deng, X. L. Xiao, L. Ding, Y. L. Yuan, H. Li, X. T. Li, X. N. Yan and L. L.
398 Wang, *Electrochim. Acta*, 2011, **56**, 4595–4602.
- 399 29 Y. Teng, L. Fan, Y. Dai, M. Zhong, X. Lu and X. Kan, *Biosens. Bioelectron.*, 2015, **71**,
400 137–142.
- 401 30 L. Zhang, J. Li, Y. Zeng, L. Meng and C. Fu, *Electroanal.*, 2015, **27**, 1–9.
- 402 31 F. Pereira, A. Fogg and M. Zanoni, *Talanta*, 2003, **60**, 1023–1032.
- 403 32 A. Vilian, S. Chen and B. Lou, *Biosens. Bioelectron.*, 2014, **61**, 639–647.
- 404 33 H. Silva, J. Pacheco, J. Silva, S. Viswanathan and C. Delerue-Matos, *Sensor. Actuat. B*,
405 2015, **219**, 301–307.
- 406 34 Z. Wang, L. Xu, G. Wu, L. Zhu and X. Lu, *J. Electrochem. Soc.*, 2015, **162**, 201–206.
- 407 35 M. B. Gholivand and N. Karimian, *Sensor. Actuat. B*, 2015, **215**, 471–479.
- 408 36 X. Tan, Q. Hu, J. Wu, X. Li, P. Li, H. Yu, X. Li and F. Lei, *Sensor. Actuat. B*, 2015, **220**,
409 216–221.
- 410 37 J. Luo, S. Jiang and X. Liu, *Sensor. Actuat. B*, 2014, **203**, 782–789.
- 411 38 X. Tan, J. Wu, Q. Hu, X. Li, P. Li, H. Yu, X. Li and F. Lei, *Anal. Methods*, 2015, **7**,
412 4786–4792.
- 413

414 Table 1 Determination of moxifloxacin in real samples ($n = 3$).

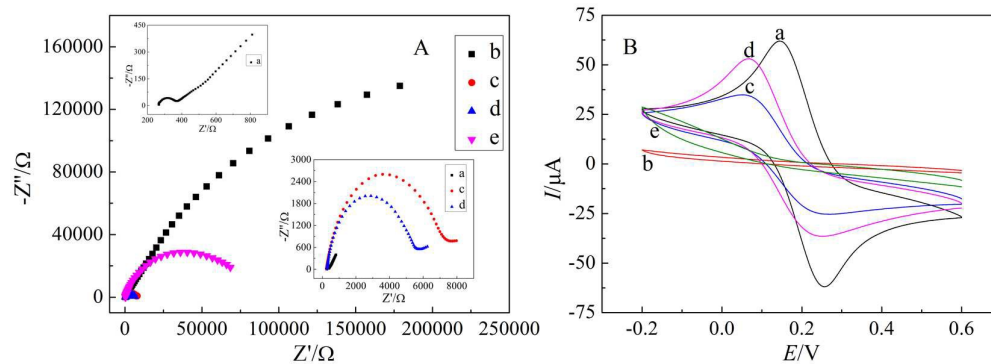
Sample	Added (μM)	Found ^a (μM)	Recovery ^b (%)	RSD ^c (%)
Tablet	0	5.36	–	1.9
	2.00	7.40	102	1.1
	4.00	9.33	99	1.3
	6.00	11.4	101	1.7
Human urine	2.00	1.91	96	0.8
	4.00	4.13	103	1.0
	6.00	5.80	97	0.6
	8.00	7.85	98	0.9

415 ^a Average value of three determinations.416 ^b Recovery (%) = (found concentration / added concentration) \times 100.417 ^c RSD: relative standard deviation.

418



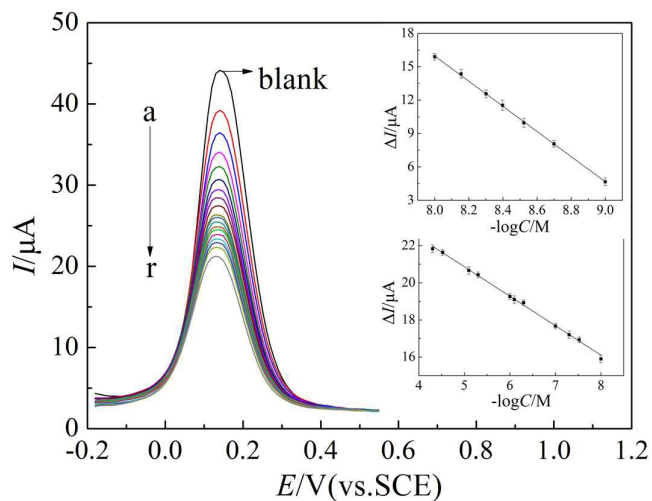
420 Fig. 1. SEM images of GR/GCE (A), MIP/GR/GCE (B) and NIP/GR/GCE (C).
421



422

423 Fig. 2. (A) EIS of different modified electrodes in 5.0 mM $\text{K}_3[\text{Fe}(\text{CN})_6]/\text{K}_4[\text{Fe}(\text{CN})_6]$
 424 containing 0.10 M KCl and (B) CV of different modified electrodes in 2.0 mM
 425 $\text{K}_3[\text{Fe}(\text{CN})_6]/\text{K}_4[\text{Fe}(\text{CN})_6]$ containing 0.10 M KCl: the bare GCE (a), MIP/GCE before elution
 426 (b), MIP/GCE after elution (c), MIP/GR/GCE after elution (d) and NIP/GR/GCE after elution
 427 (e). Insert: the bare GCE.

428

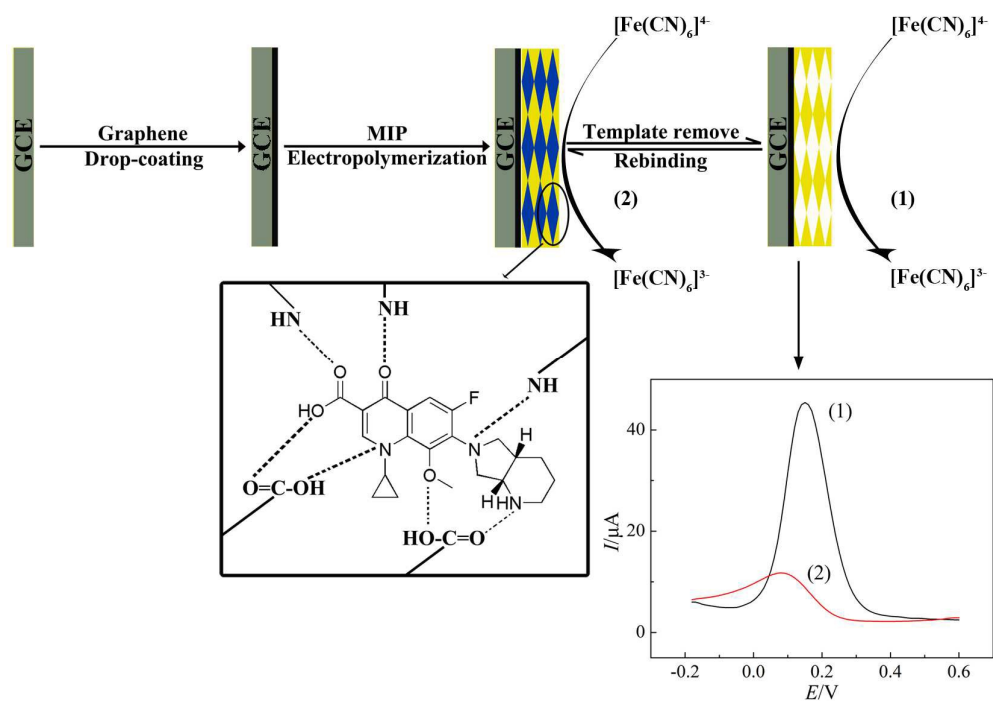


429

430 Fig. 3. Different pulse voltammograms of different moxifloxacin concentration on the sensor

431 in 2.0 mM $[\text{Fe}(\text{CN})_6]^{3-/4-}$ containing 0.10 M KCl. Insert: plot of ΔI vs. (a-r) concentration of432 moxifloxacin from 1.0×10^{-9} M to 5.0×10^{-5} M.

433



434

435 Scheme 1. Schematic illustration of stepwise electrode modification.